Aluminium doping induced enhancement of p–d coupling in ZnO



2006 J. Phys.: Condens. Matter 18 3081

(http://iopscience.iop.org/0953-8984/18/11/013)

INSTITUTE OF PHYSICS PUBLISHING JOURNAL OF PHYSICS: CONDENSED MATTER

J. Phys.: Condens. Matter **18** (2006) 3081–3087 doi:10.1088/0953-8984/18/11/013

# Aluminium doping induced enhancement of p–d coupling in ZnO

**G W Cong[1,4], W Q Peng[1], H Y Wei[1], X L Liu[1], J J Wu[1], X X Han[1], Q S Zhu[1], Z G Wang[1], Z Z Ye[2], J G Lu[2], L P Zhu[2], H J Qian[3], R Su[3], C H Hong[3], J Zhong[3], K Ibrahim[3] and T D Hu[3]**

[1] Key Laboratory of Semiconductor Materials Science, Institute of Semiconductors, Chinese Academy of Sciences, PO Box 912, Beijing 100083, People's Republic of China
[2] State Key Laboratory of Silicon Materials, Zhejiang University, Hangzhou 310027, People's Republic of China
[3] Beijing Synchrotron Radiation Facility, Institute of High Energy Physics, Chinese Academy of Sciences, PO Box 918, Beijing 100039, People's Republic of China

E-mail: gwcong@semi.ac.cn

Received 27 July 2005, in final form 30 September 2005
Published 1 March 2006
Online at stacks.iop.org/JPhysCM/18/3081

**Abstract**

Valence-band type Auger lines in Al doped and undoped ZnO were comparatively studied with the corresponding core level x-ray photoelectron spectrography (XPS) spectra as references. Then the shift trend of energy levels in the valence band was that p and p–s–d states move upwards but e and p–d states downwards with increasing Al concentration. The decreased energy of the Zn 3d state is larger than the increased energy of the O 2p state, indicating the lowering of total energy. This may indicate that Al doping could induce the enhancement of p–d coupling in ZnO, which originates from stronger Al–O hybridization. The shifts of these states and the mechanism were confirmed by valence band XPS spectra and O K-edge x-ray absorption spectrography (XAS) spectra. Finally, some previously reported phenomena are explained based on the Al doping induced enhancement of p–d coupling.

## 1. Introduction

The importance of cation outer d states in II–VI semiconductors was first discussed by Wei and Zunger [1] and subsequently confirmed by theoretical investigations [2–4]. These cation d states play a non-negligible role in electronic structures by coupling with anion p states [1–4]. This p–d coupling has been proved to be influential to some important properties, such as lattice constant, bandgap and band offsets [1, 2, 5, 6]. Thus the change of p–d coupling will influence the optical and electrical properties of II–VI semiconductors. Zinc oxide (ZnO)

[4] Author to whom any correspondence should be addressed.

is an important II–VI semiconductor due to its potential applications in short-wavelength optoelectronic devices [7, 8], nanodevices [9, 10], and field emission devices [11]. In the *ab initio* calculations of the electronic structure for ZnO [2, 12, 13], results more consistent with experiments were obtained when Zn 3d electrons were included in the valence band (VB) together with O 2p electrons. The presence of p–d coupling in ZnO was also supported by experiments [13, 14]. However, the response of p–d coupling to extrinsic doping has been rarely discussed, which is meaningful from aspects of physics and applications. This paper is in response to such an objective by analysing the Auger line shape of Al doped and undoped ZnO. Al is a good dopant to realize n-type ZnO [15]. Different concentrations of Al are doped into ZnO films to discern the corresponding change of p–d coupling. The effect of Al doping on p–d coupling may provide a new explanation for some observed but unclear phenomena in ZnO.

## 2. Experiment

Undoped and Al doped ZnO films (in varied atomic ratio [Al]/[Zn] of 1%, 2%, and 4%) of about 640 nm thickness were deposited on glass substrates by DC magnetron sputtering. The sputtering gas was highly pure $O_2$ (99.99%) mixed with highly pure Ar (99.99%). Deposition was performed for 30 min under a constant substrate temperature (500 °C) with a constant pressure of 5 Pa. Finally, these epilayers underwent an annealing process under higher temperature in oxygen to realize crystallization. Auger lines as well as x-ray photoelectron spectrography (XPS) spectra were recorded on a VG MKII XPS instrument with Al K$\alpha$ ($h\nu = 1486.6$ eV) as the x-ray source, which had been carefully calibrated on the work function and Fermi energy level ($E_F$). All spectra were accumulatively scanned six times with a step of 0.15 eV per 100 mS and calibrated by the C 1s peak from contamination. X-ray absorption spectrography (XAS) spectra at the O K edge were measured at the photoemission station of Beijing Synchrotron Radiation Facility. They were obtained by measuring the photocurrent directly from the samples at steps of 0.05 eV with the resolution better than 0.5 eV, which is believed to have more bulk sensitive character [16]. X-ray diffraction (XRD) measurements were performed using a Philips X'Pert x-ray generator with Cu K$\alpha_1$ radiation source ($\lambda = 0.154\,05$ nm).

All films have nearly the same XRD spectra (as shown in figure 1), which only have (0002) and (0004) diffraction peaks at 34.225° and 72.275°, respectively. This indicates the wurtzite structure of the deposited films with *c*-axis orientation. According to Hall measurements, all Al doped films show n-type conduction, and with increasing the Al doping concentration, the conductivity becomes better. For 1%, 2% and 4% Al doped ZnO films, the resistivities are 34.37, 12.54 and 1.079 Ω cm, respectively.

## 3. Auger lines and core level XPS spectra

Figures 2(a) and (b) show the Auger lines of O KLL and Zn LMM, and these Auger transition processes reflect the distribution of electron kinetic energy in the corresponding VB originating from a combination between the same VB electrons and holes in core levels. Undoubtedly the shifts of VB Auger lines can give information on the energy level structure in the VB (O 2p and Zn 3d in this case). To better analyse Auger lines, we discuss the energy levels of the VB in ZnO first. It is well known that 3d states in transition metal oxides will be split into $t_2$ and e states in the crystal field [17]. Zn 3d in ZnO is also under such splitting [1], as proved by the calculation of the density of states (DOS) in the *ab initio* calculations [2, 13]. Atoms in nearest neighbour positions of the wurtzite-structure ZnO are tetrahedrally bonded. In $T_d$

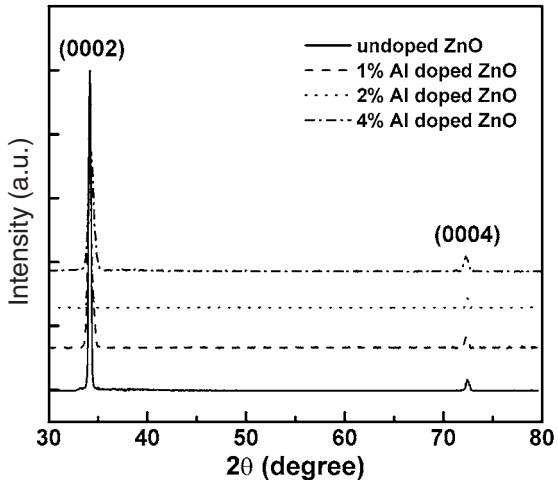


**Figure 1.** $\theta$–$2\theta$ x-ray diffraction spectra.

symmetry, Zn 3d is split into higher energy states $t_2$ and lower energy states e. O 2p undergoes splitting caused by hybridization with Zn 4s [14, 18–20]. Its splitting, caused by the crystal field and spin–orbit coupling, could be neglected in our measurements due to the very small splitting difference [21]. So O 2p is regarded approximately to be composed of hybridized and unhybridized states in this study. Considering p–d coupling, a part of the DOS from p–d coupling will be mainly incorporated into the hybridized O 2p, as proved by the wave-function analysis [2]. On the other hand, p–d coupling leads to the inversion of Zn 3d, making the states derived from p–d coupling lower than e states [1]. Calculations and experiments on the total and partial DOS have proved such an arrangement [2, 13, 22, 23]. The energy level interaction described above is exhibited in the left-hand part of figure 3. Unhybridized O 2p, hybridized O 2p incorporating p–d coupling, e states, and $t_2$ states from p–d coupling are denoted respectively as p, p–s–d, e, and p–d states. Based on such a physical picture, each spectrum in figures 2(a) and (b) can be approximately regarded to be composed of two components ($O_1$ and $Z_1$ for the low kinetic energy ones and $O_2$ and $Z_2$ for the high kinetic energy ones), consistent with the experimentally observed asymmetry. According to figure 3, $O_1$ is assigned to hybridized p–s–d states, and $O_2$ to unhybridized p states. Similarly, $Z_1$ is related to p–d states and $Z_2$ to e states. It can be seen that O KLL does not show an apparent position shift with increasing Al concentration, but the components $Z_1$ and $Z_2$ in Zn LMM both shift to lower kinetic energy, by $\sim$2.85 and $\sim$3.1 eV, respectively, compared to the undoped ZnO.

It is well known that the final states of Auger transitions involve core levels, O 1s and Zn 2p in this case. So O 1s and Zn 2p core level XPS spectra were measured as energy references to discuss the relative shifts of VB states. As shown in figure 2(c), both O 1s and Zn 2p shift to higher binding energy with the increase of Al concentration. For 4% Al doped ZnO with respect to undoped one, the shifts of the O 1s and Zn $2p_{3/2}$ are $\sim$1.2 and $\sim$0.9 eV, respectively. Taking the shifts of O 1s and Zn 2p into consideration, the components $O_1$ and $O_2$ are relatively energetically heightened, while $Z_1$ and $Z_2$ and lowered. Higher Al concentration results in larger downward movements of p–d and e states and upward movements of p–s–d and p states. The decreased energy for Zn 3d is larger than the increased energy for O 2p. Therefore, the p–d and e states of Al doped ZnO shift downwards by a larger amount of energy than that with which the p and p–s–d states shift upwards.

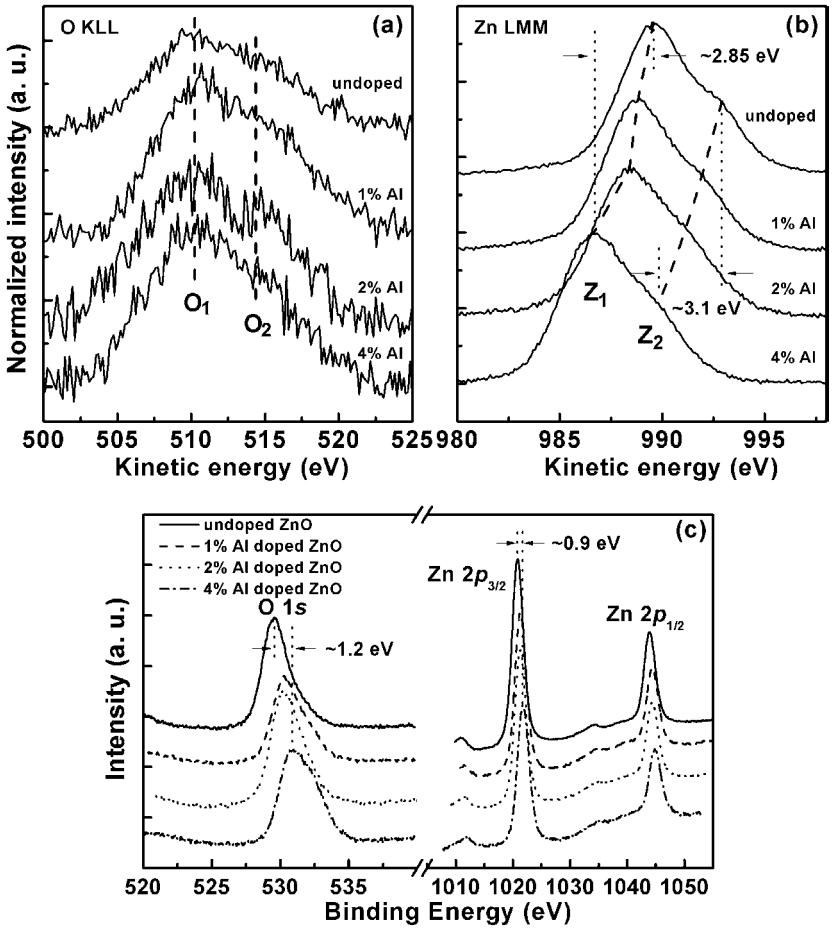


**Figure 2.** Normalized (a) O KLL and (b) Zn LMM Auger lines of undoped and Al doped ZnO. $O_1$, $O_2$ for O KLL and $Z_1$, $Z_2$ for Zn LMM are components based on the energy levels in figure 3. (c) O 1s and Zn 2p core level XPS spectra.

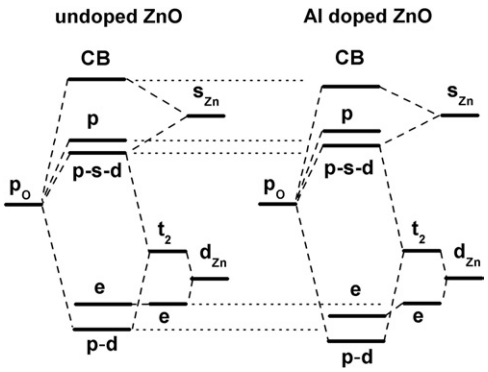


**Figure 3.** Scheme of energy level interaction in ZnO. Al doping induced enhancement of p–d coupling can be seen. CB: conduction band. The left-hand part is deduced from [1].

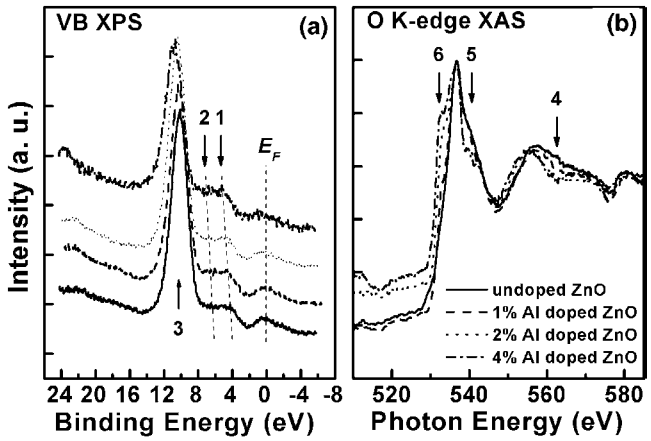


**Figure 4.** (a) VB XPS and (b) O K-edge XAS spectra. $E_F$ is given at the binding energy of zero. Each spectrum was normalized at the maximum intensity.

We describe the following mechanism to interpret the effect of Al doping. Assuming that Al occupies the substituting positions of Zn, Al–O bonds will form by s–p hybridization; these bonds have stronger bond energy and shorter bond length than Zn–O bonds. Then a number of inequivalent oxygen atoms bonded with Al atoms will come into existence. The formation of the stronger s–p hybridization in Al–O bonds will increase the DOS of p and p–s–d states. Such a change is proved by the enhancement of photoelectron intensity found for the peaks located at binding energy of ∼8 eV and ∼6 eV in Al doped ZnO with respect to undoped ZnO in [18]. When the DOS of p–s–d states increases, p–d coupling will be enhanced. Such enhanced coupling will lower the total energy and increase the energy spacing between Zn 3d and O 2p by interaction. This is consistent with the experimental results above. Then it can be concluded that Al doping may induce the enhancement of p–d coupling in ZnO films, and such coupling increases with increasing Al concentration. According to the mechanism mentioned above, the enhancement of p–d coupling should result from the addition of a new DOS into p–s–d states due to the stronger hybridization between O and Al. The result is schematically summarized in the right-hand part of figure 3.

## 4. VB XPS and XAS

To further confirm the experimental results and the mechanism, both VB XPS spectra (figure 4(a)) and O K-edge XAS spectra (figure 4(b)) were recorded. In figure 4(a), the wide weak peaks around $E_F$ may be attributed to surface states or nonlocal states caused by defects. Features 1 and 2, respectively from photoelectron emission of p and p–s–d states, both slightly shift to higher binding energy with the increase of Al concentration. Feature 3, resuming from Zn 3d, combines the contribution from both e and p–d states. The splitting of Zn 3d cannot be detected by direct photoelectron emission in this case, but it can be obtained by analysing the Auger decay process. Clearly, feature 3 also shifts to higher binding energy with increasing Al concentration. It can also be seen that the energy separation between O 2p and Zn 3d slightly increases when the Al concentration increases. So the results of VB XPS support the analysis from Auger lines in section 3. As predicted by the mechanism aforementioned, inequivalent oxygen sites will come into existence due to the bonding with Al atoms and stronger s–p hybridization between Al and O leads to the increase of the DOS of p–s–d states. Then new

unoccupied DOS derived from such hybridization will be incorporated into the conduction band. The existence of inequivalent oxygen sites and the unoccupied DOS related to O 2p were detected by O K-edge XAS, which depends on the scattering of the photoelectron wave from neighbouring atoms so as to reflect the local structure around the absorber and the information of unoccupied states. As shown in figure 4(b), all XAS spectra have similar line shapes and match previously published XAS spectra for ZnO nanostructures [13, 20]. The absorption peak is located at the photon energy of ∼537 eV. In the region above 537 eV, the x-ray absorption can be mainly assigned to O 2p–Zn 4p and O 2p–Zn 4d hybridized states [13, 20]. In the region of ∼531–537 eV, apparent absorption edges were observed. The contribution in the absorption edge mainly comes from O 2p–Zn 4s hybridized states. The absorption edge of Al doped ZnO slightly moves to lower photon energy compared with that of undoped ZnO, reflecting the downward movement of the conduction band minimum. Considering the upward movement of p and p–s–d states, this manifests the reduction of bandgap for Al doped ZnO, which is also shown in the right part of figure 3. Features 4, 5 and 6 denote the main differences caused by the variation of Al concentration. These show that increasing the Al concentration results in several sharper spectral features, an indication of the increase in O 2p state localization. The increase in relative intensity of feature 6 indicates the increase of the unoccupied DOS of O 2p–Zn 4s hybridized states. This phenomenon is in accordance with the prediction that the new unoccupied DOS caused by strong s–p hybridization of Al–O bonds will be incorporated into the conduction band. These phenomena above should be directly related to the inequivalent oxygen sites caused by stronger s–p hybridization in Al–O bonds, making O 2p more localized and increasing the unoccupied DOS. Therefore, the mechanism we used to interpret Al doping induced enhancement of p–d coupling is confirmed.

Al doping induced enhancement of p–d coupling in ZnO can be applied to further clarify some previously reported phenomena. An upward VB edge shift for 3% Al doped ZnO was interpreted as the reduction of the bandgap, indicating no semiconductor–metal transition upon Al doping for ZnO [18]. We observed the red shift of the absorption edge for Al–N codoped ZnO with respect to N doped ZnO [24]. Al doping induced enhancement of p–d coupling may reduce the bandgap, giving a fundamental reason for such observations. The III–V codoping method is regarded as a feasible way to produce p-type ZnO [22]. However, a very puzzling result can be found in that the presence of III group elements enhanced the carrier concentration as predicted, but the hole mobility was decreased by as much as an order of magnitude [24–26]. Besides the possible new scattering caused by III group elements, the decrease of mobility could also be understood from the energy level structure. It is suggested that Al doping induced enhancement of p–d coupling may prefer to make the hole level more localized, as the presence of more localized O 2p shows in figure 4(b).

## 5. Conclusions

In summary, Al doping can induce the enhancement of p–d coupling in ZnO in terms of the analysis of O KLL and Zn LMM Auger lines as well as O 1s and Zn 2p core level XPS spectra. Such an enhancement should result from the stronger Al–O hybridization. The increase of Al concentration results in stronger p–d coupling, further separating O 2p and Zn 3d. This was confirmed by VB XPS spectra and O K-edge XAS spectra. Finally, Al doping induced enhancement of p–d coupling was adopted to explain some phenomena.

## References

[1] Wei S-H and Zunger A 1988 *Phys. Rev.* B **37** 8958
[2] Schröer P, Krüger P and Pollmann J 1993 *Phys. Rev.* B **47** 6971

[3] Schröer P, Krüger P and Pollmann J 1994 *Phys. Rev.* B **49** 17092
[4] Vogel D, Krüger P and Pollmann J 1995 *Phys. Rev.* B **52** R14316
[5] Wei S-H and Zunger A 1998 *Appl. Phys. Lett.* **72** 2011
[6] Segev D and Wei S-H 2003 *Phys. Rev.* B **68** 165336
[7] Tsukazaki A, Ohtomo A, Onuma T, Ohtani M, Makino T, Sumiya M, Ohtani K, Chichibu S F, Fuke S, Segawa Y, Ohno H, Koinuma H and Kawasaki M 2005 *Nat. Mater.* **4** 42
[8] Tang Z K, Wong G K L, Yu P, Kawasaki M, Ohtomo A, Koinuma H and Segawa Y 1998 *Appl. Phys. Lett.* **72** 3270
[9] Huang M H, Mao S, Feick H, Yan H, Wu Y, Kind H, Weber E, Russo R and Yang P 2001 *Science* **292** 1897
[10] Kong X Y, Ding Y, Yang R S and Wang Z L 2004 *Science* **303** 1348
[11] Cheng J, Guo R and Wang Q M 2004 *Appl. Phys. Lett.* **85** 5140
[12] Kohan A F, Ceder G, Morgan D and Van de Walle C G 2000 *Phys. Rev.* B **61** 15019
[13] Dong C L, Persson C, Vayssieres L, Augustsson A, Schmitt T, Mattesini M, Ahuja R, Chang C L and Guo J-H 2004 *Phys. Rev.* B **70** 195325
[14] Girard R T, Tjernberg O, Chiaia G, Söderholm S, Karlsson U O, Wigren C, Nylén H and Lindau I 1997 *Surf. Sci.* **373** 409
[15] Kim K-K, Niki S, Oh J-Y, Song J-O, Seong T-Y, Park S-J, Fujita S and Kim S-W 2005 *J. Appl. Phys.* **97** 066103
[16] Ibrahim K, Qian H J, Wu X, Abbas M I, Wang J O, Hong C H, Su R, Zhong J, Dong Y H, Wu Z Y, Wei L, Xian D C, Li Y X, Lapeyre G J, Mannella N, Fadley C S and Baba Y 2004 *Phys. Rev.* B **70** 224433
[17] De Groot F M F, Grioni M, Fuggle J C, Ghijsen J, Sawatzky G A and Peterson H 1989 *Phys. Rev.* B **40** 5715
[18] Gabás M, Gota S, Ramos-Barrado J R, Sánchez M, Barrett N T, Avila J and Sacchi M 2005 *Appl. Phys. Lett.* **86** 042104
[19] Perkins C L, Lee S-H, Li X, Asher S E and Coutts T J 2005 *J. Appl. Phys.* **97** 034907
[20] Chiou J W, Jan J C, Tsai H M, Bao C W, Pong W F, Tsai M-H, Hong I-H, Klauser R, Lee J F, Wu J J and Liu S C 2004 *Appl. Phys. Lett.* **84** 3462
[21] Mang A, Reimann K and Rübenacke St 1995 *Solid State Commun.* **94** 251
[22] Yamamoto T and Yoshida H K 1999 *Japan. J. Appl. Phys.* 2 **38** 166
[23] McGuinness C, Stagarescu C B, Ryan P J, Downes J E, Fu D, Smith K E and Egdell R G 2003 *Phys. Rev.* B **68** 165104
[24] Lu J G, Ye Z Z, Zhuge F, Zeng Y J, Zhao B H and Zhu L P 2004 *Appl. Phys. Lett.* **85** 3134
[25] Singh A V, Mehra R M, Wakahara A and Yoshida A 2003 *J. Appl. Phys.* **93** 396
[26] Joseph M, Tabata H and Kawai T 1999 *Japan. J. Appl. Phys.* **38** L1205